Frontiers in Heat Pipes

Available at www.ThermalFluidsCentral.org

TEMPERATURE UNIFORMITY ANALYSIS OF A MULTI-WELL VAPOR CHAMBER HEAT SPREADER

Shung-Wen Kang[a*], Yu-Tang Chen[b], Chun-Hsiang Hsu[a] and Jun-Ying Lin[a]

[a] Mechanical and Electro-Mechanical Engineering, Tamkang University, Tamsui Dist., New Taipei City, 25137, Taiwan(R.O.C)
[b] Department of Mechanical Engineering, De Lin Institute of Technology, Tucheng Dist., New Taipei City, 236, Taiwan(R.O.C)

ABSTRACT

In this study, temperature uniformity and heating rate of heat spreader with multi-well are simulated and analyzed by CFD software under natural convection condition. Firstly, multi-well heat spreader made of aluminum, copper, silver and vapor chamber are simulated and compared, when dual and six heat sources are applied at a heating power of 1200W. Secondly, with six heat sources at heating power of 188, 300, 600 and 1200W, the heating rate of heat spreaders are studied. Vapor chamber heat spreader has the better temperature uniformity both in six sources and dual sources mode due to a higher thermal conductivity, followed by silver, copper and aluminum heat spreader. Aluminum and silver heat spreader show the higher heating rate, followed by copper heat spreader, vapor chamber heat spreader due to a larger heat capacity, heat up the slowest.

Keywords: Multi-well heat spreader, Heating rate, Temperature uniformity, Vapor chamber

1. INTRODUCTION

The polymerase chain reaction, PCR, was invented by K. Mullis, and includes three basic reactions, denature, annealing, and extension (Adams *et al.*, 2005), all of which have corresponding temperatures, range of temperatures, periods of reaction, and temperature uniformity. As these reactions absolutely influence the final products (Zhang and Xing, 2007), it is important to reduce the period of reaction and raise temperature uniformity. Many domestic and foreign researches are based on micro chips, which use MEMS technology or micro-tunnel polymerase chain reaction biochips (Singh and Ekaputri, 2006; Kreith and Bohn, 2001; Shen and Chen, 2005). Even though, the situation of a reduced area raises temperature uniformity to ± 0.5°C, the cost is high and the situation is not available for mass production. In this research, the size of the multi-well heat spreader is four times that of a micro chip and utilizes the temperature uniformity of a vapor chamber heat spreader, which allows simultaneous operations, in order to meet the needs of PCR.

A Vapor Chamber is a closed hollow object that is full of working fluid, with an inner vacuum pump. The purpose of vacuum pumping is to reduce the boiling point of the working fluid, which makes it easier to achieve the phase transition that allows heat to spread rapidly (Kang *et al.* 2010; Tsai *et al.* 2010; Kang and Huang, 2008). Thermacore, Inc. (2000) simulated copper fins, which they compared with a vapor chamber combined with copper fins. The results show that copper fins have the obvious phenomena of centralizing the heat sources, which can easily generate a situation of uneven temperature; in contrast, a vapor chamber with copper fins has even temperature distribution. Currently, vapor chamber heat spreaders apply electronic cooling, which meet the high requirements of even temperatures in biomedical technology.

This research applies a basic simulation and analysis with copper, aluminum, silver, and vapor chamber heat spreaders. First, we change the number of heat sources, with a fixed heating power of 1200W, and simulate temperature distribution where the heating center of dual and six heating sources on a multi-well heat spreader is from room temperature to 90°C. This study uses six heat sources to operate simulations at different heating speeds of 188, 300, 600, and 1200W, observes the period of reaction and speed of warming, and discusses the a multi-well vapor chamber heat spreader in the conclusion.

2. CFD SIMULATION

2.1 Simulating the model of machine

Figure 1 shows a simplified model of the test equipment, which includes a multi-well vapor chamber heat spreader, heat sources, and cooling fins, which is an exact size according to actual measurements. As this study only simulates the situation of warming in the machine, we simplified the model and ignored fans, nozzle shaped fins, and fan cover.
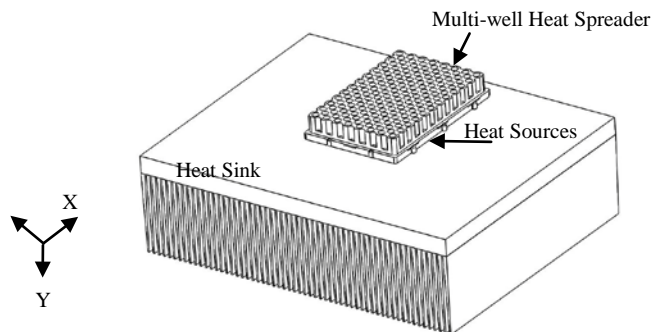

Fig. 1 The model of test equipment

*Corresponding author. Email: swkang@mail.tku.edu.tw

1. Multi-well vapor chamber heat spreader (112×75×17.2mm): Figure 2 is composed of a vapor chamber heat spreader (thickness 4mm), with 96 holes (diameter of the holes is 5mm and depth is 10mm).
2. Heat sources: the area of heat sources is 30×30mm. Based on simplified modeling, the heat sources is 2D, and assumes that heat generation is even.
3. Cooling fins (250×200×73mm): the thickness of the substrate is 13mm, the fins are nozzle shaped, the thickness of the substrate is 2mm, and the bottom is 1mm, as seen in Figure 3. In addition, the fins have 17 hollow cylinders, with a diameter of 13mm, and are located in the area with the multi-well heat spreader to allow the multi-well heat spreader, heat sources, and cooling fins to fully cooperate; as the actual nozzle fins are difficult to model, the simulation has simplified fins, with the single size of 1.5mm.
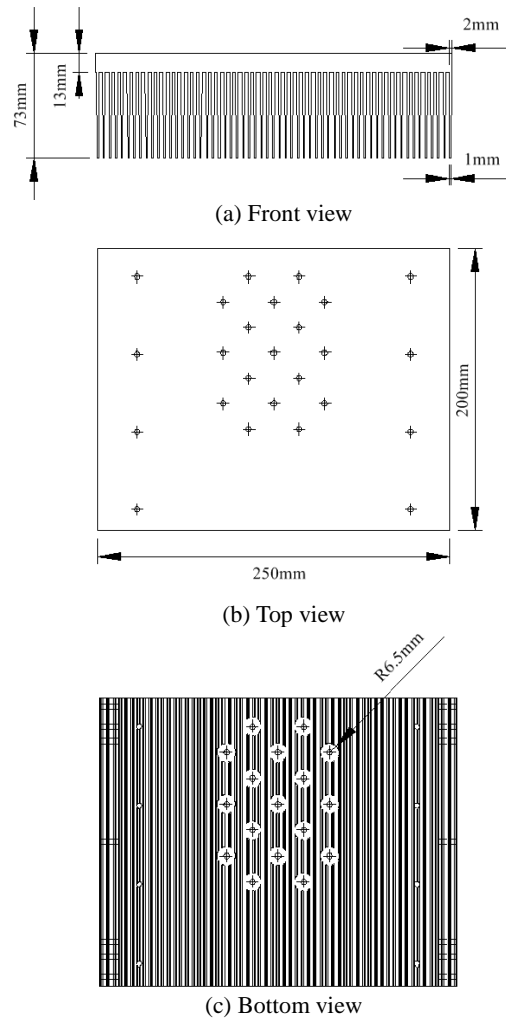
2.2 Exact Formula

Mass-conservation equation, i.e.:

$$\frac{\partial u}{\partial x} + \frac{\partial v}{\partial y} + \frac{\partial w}{\partial z} = 0$$

Momentum conservation equation, i.e.:

$$\rho\left(\frac{\partial u}{\partial t} + u\frac{\partial u}{\partial x} + v\frac{\partial u}{\partial y} + w\frac{\partial u}{\partial z}\right) = \rho g_x - \frac{\partial p}{\partial x} + \mu\left(\frac{\partial^2 u}{\partial x^2} + \frac{\partial^2 u}{\partial y^2} + \frac{\partial^2 u}{\partial z^2}\right)$$

$$\rho\left(\frac{\partial v}{\partial t} + u\frac{\partial v}{\partial x} + v\frac{\partial v}{\partial y} + w\frac{\partial v}{\partial z}\right) = \rho g_y - \frac{\partial p}{\partial y} + \mu\left(\frac{\partial^2 v}{\partial x^2} + \frac{\partial^2 v}{\partial y^2} + \frac{\partial^2 v}{\partial z^2}\right)$$

$$\rho\left(\frac{\partial w}{\partial t} + u\frac{\partial w}{\partial x} + v\frac{\partial w}{\partial y} + w\frac{\partial w}{\partial z}\right) = \rho g_z - \frac{\partial p}{\partial z} + \mu\left(\frac{\partial^2 w}{\partial x^2} + \frac{\partial^2 w}{\partial y^2} + \frac{\partial^2 w}{\partial z^2}\right)$$

Energy conservation equation, i.e.:

$$\frac{\partial}{\partial t}(\rho h) = \nabla \cdot (k\nabla T) + S_h$$

where ρ denotes density, u, v, and w are velocity components, p denotes pressure, μ denotes the viscosity coefficient, g denotes gravity, and h denotes enthalpy.
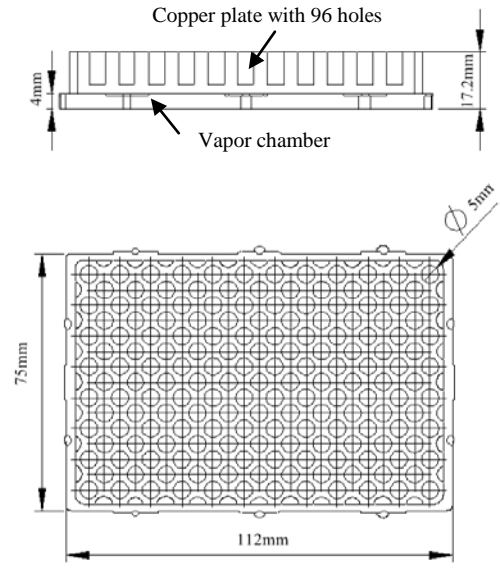

Fig. 2 The size of multi-well vapor chamber heat spreader

(a) Front view

(b) Top view

(c) Bottom view

Fig. 3 The size of cooling fins

In the natural convection, we used a Rayleigh number to calculate the intensity of buoyant force. i.e.:

$$Ra = \frac{g\beta\beta\Delta T^3\rho}{\mu\alpha}$$

ANSYS Icepak uses the Boussinesq model in the natural convection. All of the equations, with the exception of the momentum equation's buoyant force, assume that density is an identical value. i.e.:

$$(\rho - \rho_0)g \approx -\rho_0\beta(T - T_0)g$$

where ρ_0 is the density of the fluid, which is an identical value; T0 is the temperature of operation.

2.3 Convergence Test

This article sets the convergence of momentum and energy at 10-1, 10-2, and 10-3 in order to maintain the solution in a steady state, and the solution of 10-2 is close to 10-3, and in both of the two situations, energy can weaken to 10-7; therefore, this research set the convergence of momentum at 10-2, and the convergence of energy at 10-7.

2.4 The relaxation factor

As this article intends to resolve the process of transient heating in natural convection, to make the process easier, we set the relaxation factor at 0.7, and the momentum relaxation factor at 0.1, in order to

complete the solution. It symbolizes that the difference of pressure from one iteration to the next will be limited under 70%, and the change of momentum will be limited under 10%.

3. RESULTS AND DISCUSSION

3.1 Comparisons of experiments

The simulated test equipment, under heating powers of 188w and 288w, and with dual or six heating sources, are compared for temperature distribution and time, with results as shown in Fig. 4 and 5. The results of the simulations are limited to these experiments, under dual or six heat source situations, with the temperature maintained at 90°C, the deviation becomes very low, approximately 1.72%.
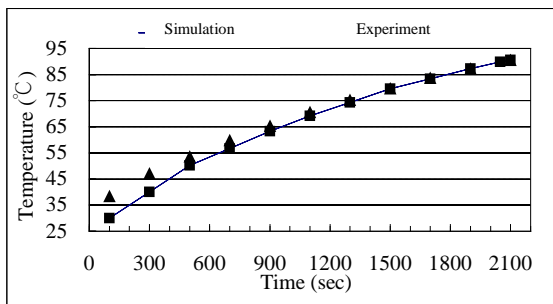
Fig. 4 The comparison of the simulation and experiment with six heat sources in a copper heat spreader
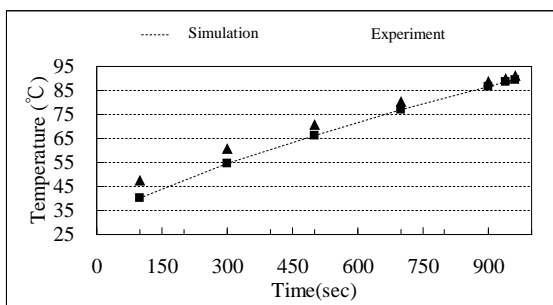

Fig. 5 The comparison of the simulation and experiment of dual heat sources with a copper heat spreader

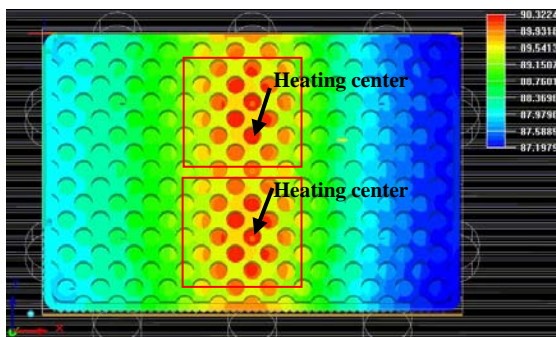### 3.2 Analysis with dual and six heat sources temperature uniformity

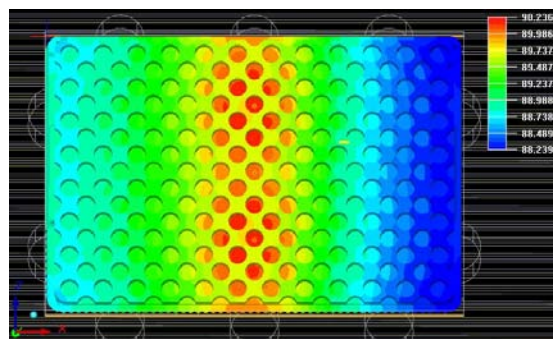**Fig. 6** Temperature distribution of aluminum vapor chamber under dual sources (ΔT=3.12 °C)

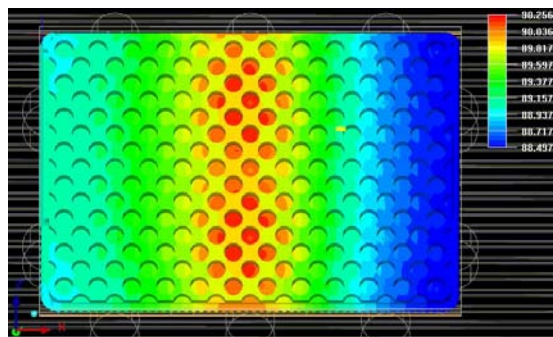**Fig. 7** Temperature distribution of copper vapor chamber under dual sources (ΔT=2.00 °C)

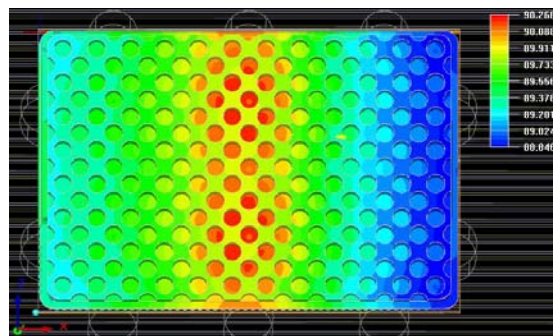**Fig. 8** Temperature distribution of silver vapor chamber under dual sources (ΔT=1.76 °C)

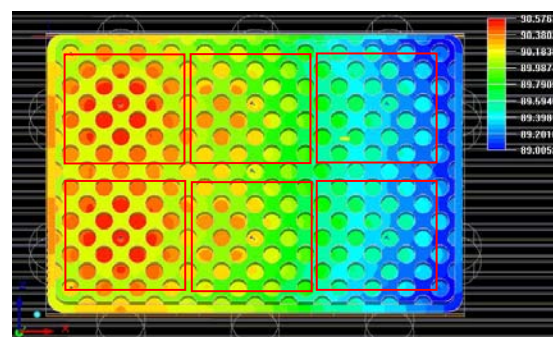**Fig. 9** Temperature distribution of vapor chamber under dual sources (ΔT=1.42 °C)

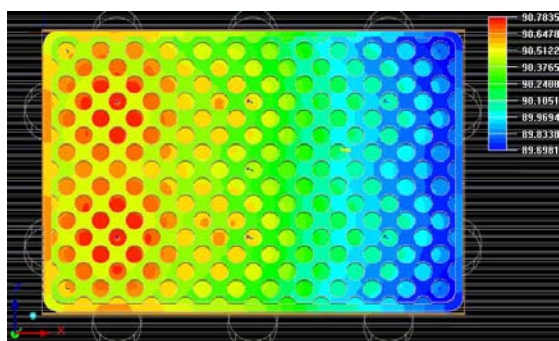**Fig. 10** Temperature distribution of aluminum vapor chamber under six sources (ΔT=1.58 °C)

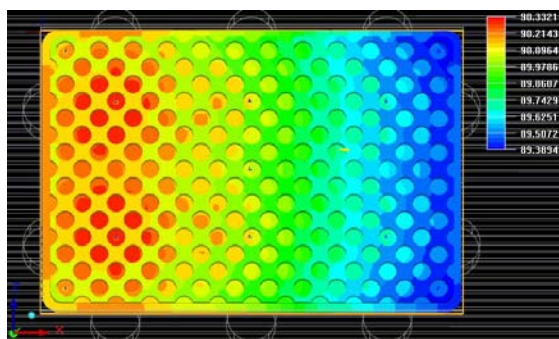**Fig. 11** Temperature distribution of copper vapor chamber under six sources (ΔT=1.09 °C)

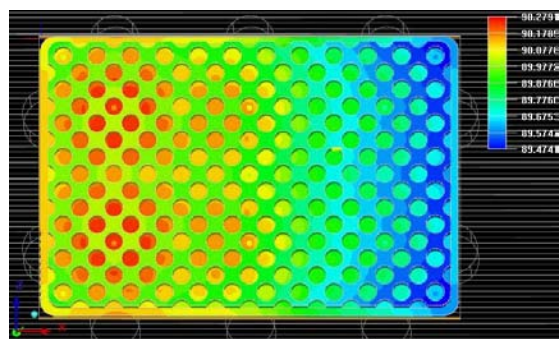**Fig. 12** Temperature distribution of copper vapor chamber under dual sources (ΔT=0.94 °C)

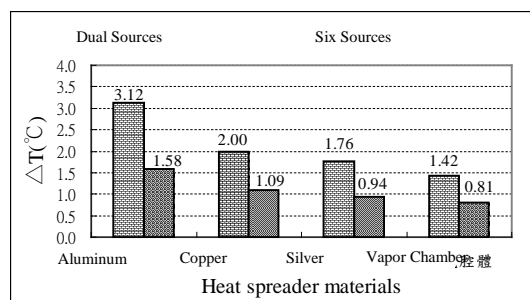**Fig. 13** Temperature distribution of vapor chamber under dual sources (ΔT=0.81 °C)

Fig. 14 The comparison of the temperature differential under dual and six heat sources at a heating power of 1200W

The simulation results, as shown in Figs. 6 to 13, compare the different material temperature differences, and find that when under six heat sources, the temperature difference is smaller than in dual heat sources, as shown in Fig. 14. Furthermore, the temperature uniformity is proportional to the material thermal conductivity coefficient. Thus,

temperature uniformity could be arranged as vapor chamber, silver, copper, and aluminum.

3.3 The diagram, of different heating power and the period of warming

Figure 15 shows that the simulation of the vapor chamber heat spreader requires a warming period from room temperature to 90°C when testing several heating powers of 188, 300, 600, and 1200W.
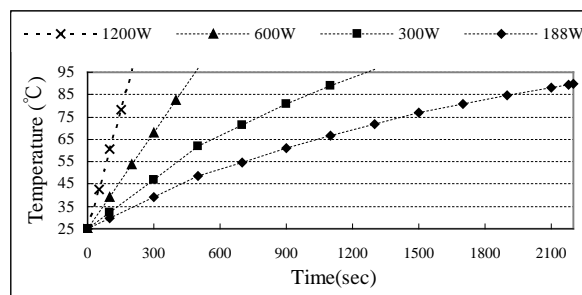

Fig. 15 The temperature distribution of the vapor chamber heat spreader at different watts

With the lower heating power, room temperature is regarded as an important parameter to influence the temperature of the heat source; therefore, the warming line is a curve. If the heating power goes lower, the steady temperature could be lower than 90°C. Prior to increasing the heating power, room temperature has no influence on the temperature of the heat source, and the line of warming tends to be a linear. Table 1 shows the detailed information, including the heating rate of several of kinds of heat spreaders with temperature uniformity.

According to the four heating speeds shown in Table 1, there are different heating rate, with different ingredients heating from room temperature to 90°C. When the temperature in the center of the heat spreader reaches 90°C, it captures the distribution of the temperature in the heat spreader. This study calculates the difference between the high and low temperatures (ΔT), as shown in Fig. 16, which shows different temperature uniformity and heating rate at 188, 300, 600, and 1200W, with different ingredients in the heat spreader. Fig. 16 compares silver, aluminum, copper and vapor chambers, the vapor chamber have the best uniformity; however, the heating speed is also the slowest. In addition, the copper has the second best uniformity, with a faster heating rate.

The heating rate in the reaction of PCR is regarded as the faster, the better, while temperature uniformity is regarded as the lower, the better; therefore, the ratio of the temperature uniformity and the heating rate is the smaller, the better. Fig. 17 presents the relationships between heat spreaders of various materials and temperature uniformity, the ratio of the heating rate, and the heating power, and shows that the ratio of a vapor chamber heat spreader's uniformity and the heating rate is lower than any other material heat spreaders. The results suggest that a vapor chamber heat spreader is the most suitable for application in the reaction of PCR.

4. CONCLUSIONS

In this study, the temperature uniformity and heating rates of heat spreaders with multi-wells were simulated and analyzed by ANSYS-Icepak software under natural convection conditions. We selected four materials for the multi-well heat spreader, including copper, aluminum, silver, and vapor chambers, as well as dual and six heating sources, at heating powers of 188, 300, 600, and 1200W, in order to simulate this research. The simulation found that, when at lower heating powers, the surrounding temperature would have great effect, thus, the temperature rise in a curve line. Otherwise, when at higher heating powers, the

effecting by the surrounding temperature is very small, so the temperature was straight up. According to the results, when under six heating sources, temperature uniformity would better than with dual sources. In addition, comparisons of temperature uniformity show that, a vapor chamber is better than silver, silver is better than copper, and copper is better than aluminum. Therefore, a multi-well vapor chamber heat spreader has better temperature uniformity than other materials.

ACKNOWLEDGEMENTS

Table 1 The material properties of heat spreaders at different watts, with six heat sources

Aluminum

Heat power (W)	Temperature differential (ΔTi)	Time (∂t)	Heating speed (ΔTi)/∂t	Temperature uniformity (ΔT)	The ratio of temperature uniformity and heating speed $\left(\dfrac{\Delta T}{\Delta Ti/\partial t}\right)$
188	65	2175	0.030	0.504	16.861
300	65	1070	0.061	0.782	12.866
600	65	444	0.146	0.983	6.714
1200	65	185	0.351	1.584	4.509

Copper

Heat power (W)	Temperature differential (ΔTi)	Time (∂t)	Heating speed (ΔTi)/∂t	Temperature uniformity (ΔT)	The ratio of temperature uniformity and heating speed $\left(\dfrac{\Delta T}{\Delta Ti/\partial t}\right)$
188	65	2184	0.030	0.299	10.056
300	65	1076	0.060	0.404	6.683
600	65	437	0.149	0.725	4.871
1200	65	192	0.339	1.085	3.206

Silver

Heat power (W)	Temperature differential (ΔTi)	Time (∂t)	Heating speed (ΔTi)/∂t	Temperature uniformity (ΔT)	The ratio of temperature uniformity and heating speed $\left(\dfrac{\Delta T}{\Delta Ti/\partial t}\right)$
188	65	2178	0.030	0.249	8.337
300	65	1080	0.060	0.410	6.819
600	65	421	0.154	0.713	4.617
1200	65	182.5	0.356	0.943	2.647

Vapor chamber

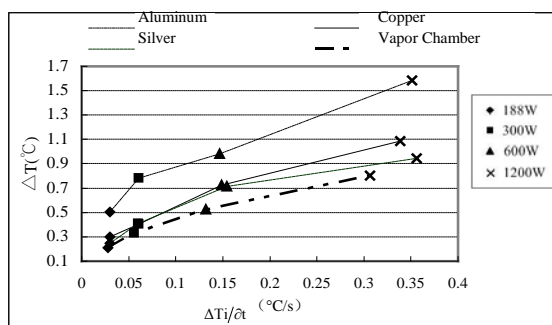| Heat power (W)	Temperature differential (ΔTi)	Time (∂t)	Heating speed (ΔTi)/∂t	Temperature uniformity (ΔT)	The ratio of temperature uniformity and heating speed $\left(\dfrac{\Delta T}{\Delta Ti/\partial t}\right)$
188	65	2330	0.028	0.208	7.456
300	65	1166	0.056	0.331	5.941
600	65	492	0.132	0.526	3.983
1200	65	212.2	0.306	0.805	2.628

Fig. 16 The temperature uniformity and heating speed of the heat spreader with different watts and different materials
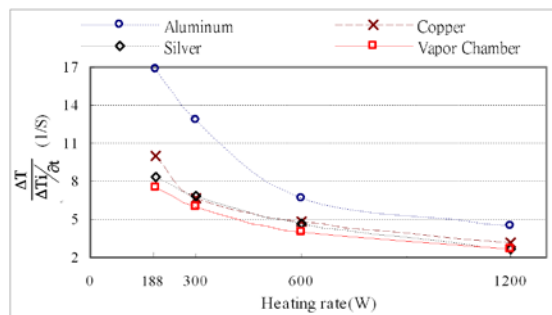

Fig. 17 The ratio of the temperature uniformity and heating rate with different watts and different materials

REFERENCE

Adams, S., and Russ, C. Uribe, M., Marincola, F.M., Stroncek, D., 2005, "PCR Validation Testing Utilizing a Novel Dynamic Measurement System," Cultech, Inc.

Icepak 4.1 User's Guide, August 2003.

Kang, S. W., Hung, Y. H., 2008, "Feasibility study of an aluminum vapor chamber," *Proceeding of 9th International Heat Pipe Symposium*, Malaysia, pp. 103-106.

Kang, S. W., Yu, C. S., Weng, M. T., 2010, "Effective thermal management of multiple electronic components," *IMPACT 2010 & International 3D IC Conference*, Taipei, Oct. 20-22.

Kreith, F., Bohn, M.S., 2001, "Principles of Heat Transfer," 6th Edition, Brooks/Cole, Pacific Grove, California.

Shen, K., Chen, X., 2005, "A microchip-based PCR device using flexible printed circuit technology," *Sensors and Actuators B*, vol. 105, pp. 251-258.
http://dx.doi.org/10.1016/j.snb.2004.05.069

Singh, J., Ekaputri, M., 2006, "PCR thermal management in an integrated Lab on Chip," *J. Phys.-Conf. Series*, **34**, 222–227.

Thermacore, Inc., "Therma-BaseTM Heat Sink", 2000.

Tsai, M. C., Yu, C.S., Kang, S. W., 2010, "A Large Size Vapor Chamber Used on Multiple Heat Sources Blade Server System," *15th International Heat Pipe Conference*, Clemson, SC, April 25-30.

Tsai, M. C., Chien, K. C., Huang, C. Y., Kang, S. W., 2008, "Thermal Performance of a Vapor Chamber," *9th International Heat Pipe Symposium*, Malaysia, pp. 86-89.

Zhang, C., Xing, D., 2007, "SURVEY AND SUMMARY Miniaturized PCR chips for nucleic acid amplification and analysis: latest advances and future trends," *Nucleic Acids Research*, Vol. 35, No. 13, 4223–4237.
http://dx.doi.org/10.1093/nar/gkm389